Technical Report

March 6, 2026

Mortality and morbidity in Switzerland under a changing climate

A report to the National Centre for Climate Services

Veruska Muccione, Abbas Mirmashhouri and Saeid Ario Vaghefi



University of Zurich[UZH]

E Clim

Abstract

This technical report assesses how climate change may affect heat-related mortality and emergency hospital admissions (EHA) in Switzerland and explores how a stylised form of adaptation could modify these impacts. Using national daily mortality (1995–2019) and EHA data (1998–2019) for the warm season (May to September), the analysis estimates non-linear temperature–health relationships within a distributed lag framework and defines impacts relative to the minimum mortality/morbidity temperature (MMT). These empirically derived relationships are then combined with transient CH2018 climate scenarios (2020–2069) under RCP2.6, RCP4.5, and RCP8.5, using multiple climate-model chains. Heat-attributable mortality is calculated with an attributable fraction formulation, and morbidity impacts are derived with a simplified attributable fraction formulation.

Projections show a clear scenario-dependent rise in heat-related mortality by mid-century, with older adults (over 75 years old) accounting for most of the absolute burden across all scenarios. For all ages combined and without adaptation, median cumulative heat-related deaths over 2050–2069 increase from 5116 in the reference period (2000–2019) to 7846 under RCP2.6, 13330 under RCP4.5, and 17755 under RCP8.5, with uncertainty ranges widening markedly in higher-warming scenarios. In contrast, projected heat-related EHAs increase more modestly: from 17,664 in the reference period to 19208 (RCP2.6), 19367 (RCP4.5), and 19511 (RCP8.5). Age-stratified results indicate the largest relative increase in children (0–14 years), while adults (15–64 years) contribute the largest absolute number of admissions. A temperature-dependent logistic adaptation function substantially reduces projected mortality and moderates morbidity outcomes, indicating that adaptation could offset a considerable share of future heat impacts. However, because adaptation is represented as a stylised sensitivity scenario rather than being tied to specific interventions or observed trends, results should be interpreted as illustrating plausible ranges and levers for risk reduction rather than as forecasts of achievable benefits.

Contents

1 Background **1**

2 Introduction **2**

3 Methods **4**
3.1 Health and climate data 4
3.1.1 Estimation of the temperature health associations 5
3.2 Attributable Fraction 7
3.2.1 Mortality approach 7
3.2.2 Morbidity approach 8
3.2.3 Baseline period health impacts 8
3.3 Projected mortality and morbidity 8
3.3.1 Mortality projections 9
3.3.2 Morbidity projections 9
3.4 Adaptation scenarios 10
3.5 Uncertainty quantification 12

4 Results **13**
4.1 Relative Risk and Projected Trends 13
4.2 Mortality and Morbidity counts 19

5 Discussion **23**

6 Conclusions **26**

List of Figures

4.1 **Smoothed relative risks (RR) of mortality are shown as a function of daily maximum temperature**. The green dashed vertical line indicates the minimum mortality temperature (MMT) for each canton, and the red dashed horizontal line represents $RR = 1$ (reference risk). The cantons are from top clockwise: BS=Basel Stadt, BE = Bern, VD = Vaud, ZH = Zurich. 14

4.2 **Decade-averaged relative risk trends for mortality under different climate scenarios in four Swiss cantons (BS, BE, VD, ZH)**. Average relative risks (RR) are shown for the period 2020–2070 under RCP2.6 (green), RCP4.5 (orange), and RCP8.5 (red). Values represent decade-averaged projections. The cantons are from top to bottom: BS=Basel Stadt, BE = Bern, VD = Vaud, ZH = Zurich. . . . 16

4.3 **Smoothed relative risks (RR) of morbidity are shown as a function of daily maximum temperature**. The green dashed vertical line indicates the minimum morbidity temperature (MMT) for each canton, and the red dashed horizontal line represents RR = 1 (reference risk). The cantons are from top clockwise: BS=Basel Stadt, BE = Bern, VD = Vaud, ZH = Zurich. 17

4.4 **Decade-averaged relative risk trends for morbidity under different climate scenarios in four Swiss cantons (BS, BE, VD, ZH)**. Average relative risks (RR) are shown for the period 2020–2070 under RCP2.6 (green), RCP4.5 (orange), and RCP8.5 (red). Values represent decade-averaged projections. The cantons are from top to bottom: BS=Basel Stadt, BE = Bern, VD = Vaud, ZH = Zurich. . . 18

List of Tables

4.1 **Heat related deaths stratified by age group**. Projected number of heat-related deaths (median) in Switzerland by age group under different emission scenarios. Values are cumulative counts over 20 years; brackets indicate the (10^{th} and 90^{th} percentiles. 19
4.2 **Heat related deaths aggregated**. Projected heat-related deaths in Switzerland for all age groups combined under RCP2.6, RCP4.5 and RCP8.5. Results are shown without adaptation and with adaptation. Values represent cumulative deaths over 20 years (2050–2069) compared with the reference period (2000–2019). Brackets indicate the (10^{th} and 90^{th} percentiles uncertainty range. 20
4.3 **Heat-related emergency hospital admissions (EHA) by age group**. Heat-related emergency hospital admissions (EHA) by age group for the reference period and projected under climate scenarios RCP 2.6, RCP 4.5 and RCP 8.5. Values are point estimates; bracketed values indicate the low–high percentile range, shown on a second line within each cell. 21
4.4 **Heat-related emergency hospital admissions (EHA) aggregated**. Heat-related emergency hospital admissions (EHA) for all age groups under the reference period and climate scenarios (RCP 2.6, RCP 4.5, RCP 8.5), shown without and with adaptation. Bracketed values indicate the low–high percentile range. 22

Chapter 1

Background

This report has been produced in the context of the program Decision-making basis for dealing with climate change in Switzerland: Information on cross-sectoral issues (NCCS-Impacts) as part of the project "Costs of Climate Change in Switzerland". The project is managed by the consulting and engineering company EBP on behalf of the NCCS. This report is part of the mandate assigned by EBP to the research group Environment and Climate (Eclim) at the Department of Geography of the University of Zurich. Eclim has been mandated to assess the impacts originating from changes in the climate on human health, agriculture productivity, winter tourism and water availability and the effect of adaptation on alleviating these impacts. The present technical report details the work undertaken on the impacts of heat on human health in Switzerland without and with adaptation.

Chapter 2

Introduction

Since the 2003 European heatwave, associated with more than 70,000 excess deaths between June and September[1], Europe has experienced repeated episodes of extreme heat, including major events in 2022, 2023, and 2024, each linked to thousands of deaths [2, 3, 4]. In Switzerland, the summer of 2022 was particularly severe: an estimated 3.5% of all-cause mortality (623 deaths) was attributed to heat [5]. Importantly, about 60% of these heat-related deaths were assessed as attributable to human-induced climate change [5]. A recent modelling study of present and future mortality from non-optimal temperatures across 1,368 European regions estimated that, in Switzerland, median annual heat-related deaths during 1991–2020 were 583 (95% CI: 458–668), rising to 1,274 (95% CI: 797–1,651) under 1.5°C warming, 1,655 (95% CI: 1,142–2,331) under 2°C, and 2,907 (95% CI: 2,197–3,803) under 3°C [6].

Deaths are the most severe outcome of heat exposure, but heat also increases illness and pressure on health services. In Switzerland, approximately 1.1% of emergency hospital admissions (EHAs)—more than 31,000 admissions between 1998 and 2019 have already been attributed to above-optimal temperatures [7]. Analyses across major cantons indicate that extreme heat is associated with marked increases in admissions for urinary conditions, mental health disorders, and infectious diseases. During extreme heat episodes, the attributable fraction for dehydration-related admissions can reach 85.9%, and acute kidney injury accounts for 56.1% [7]. Across all ages, external causes constitute the largest share of heat-attributable EHAs (for example, accidents or behaviour-related causes). The leading diagnostic groups then vary by age: respiratory diseases are prominent among children aged 0–14, mental disorders among adults aged 15–64, and digestive diseases among adults aged 65 and older [7].

Heat-related impacts are increasing, particularly in urban areas due to the urban heat island effect, and among groups with heightened vulnerability such as older adults, people living with chronic cardiovascular, respiratory, renal, or mental health conditions, pregnant women, infants, children and workers exposed to

heat outdoors [8].

Against this backdrop of differential exposures and vulnerability, adaptation to heat has started gaining tracking across the European continent [9] and in Switzerland [10, 11]. Heat–health action plans (HHAPs)—sometimes termed heat prevention plans—are structured public-health interventions, often coordinated at the cantonal level in Switzerland, designed to reduce heat-related mortality and morbidity during extreme heat events [8, 12] They aim to organise a coherent response across the health and social-care system to limit the adverse impacts of rising temperatures [8, 12, 13]. In Swiss regions with more systematic HHAP implementation such as Ticino, Geneva, and Vaud heat related all cause mortality risks declined relative to regions without similarly coordinated responses [8], though attributing changes solely to HHAPs remains methodologically challenging. A persistent policy gap is ensuring that prevention measures effectively reach socioeconomically disadvantaged populations, who often remain at elevated risk despite existing interventions [8, 14].

The present study assesses changes in human mortality and emergency hospital admission (EHA) attributable to heat for different climate futures without and with adaptation. It does so by quantifying the relationship between temperature exposure and health outcomes while accounting for both the non-linear association with temperature and the delayed effects over multiple days. Finally it consider the modified association of temperature and health outcomes through the effect of a stylised approach to adaptation. The report is organised as follows: Chapter 3 describes the methodology and data used for the study; Chapter 4 presents the results, Chapter 5 discusses the findings and finally Chapter 6 outlines the main conclusions from the report and associated limitations.

Chapter 3

Methods

A DLNM-inspired distributed-lag Poisson GLM is used to assess heat-related mortality and morbidity [15, 7]. DLNMs are statistical tools used to investigate the relationship between environmental factors, such as ambient temperature, and health effects, such as mortality or hospitalizations. These models take into account the possibility that health effects may only occur after several days (delayed effects) and that the relationship between exposure and effect is not linear [16].

3.1 Health and climate data

For mortality analysis, daily death counts were obtained from Swiss Federal Office for statistics for the period 1995-2019 and stratified by two age groups, namely $<$75 and $\geq$ 75). For morbidity analysis, emergency hospital admission (EHA) data were obtained from the Swiss Federal Office for Statistics for the period 1998-2019, aggregated by canton and stratified by age groups, namely 0-14, 15-64, 65-74 and $\geq$ 75 years old. Both datasets were filtered to include only the warm season months from May through September, when heat-related health impacts are most pronounced.

To reduce the influence of outliers, health outcome data were filtered using quantile based thresholds. This is done because daily mortality and EHA occasionally show extreme peaks driven by events that are not plausibly caused by short-term temperature exposure (e.g., influenza waves, COVID-like outbreaks, reporting backlogs). Because DLNMs fit smooth non-linear relations, a small number of extreme outcome days can exert disproportionate influence and distort the estimated temperature–response and lag structure. For the main analysis, data outside the range defined by the 10^{th} and 90^{th} percentiles (quantile threshold $\theta = 0.1$) of the health outcome distribution were excluded:

$$Y_{filtered} = \{Y_d : Q_\theta(Y) < Y_d < Q_{1-\theta}(Y)\} \tag{3.1}$$

where $Q_\theta(Y)$ represents the θ-th quantile of the health outcome distribution. Temperature data were similarly filtered to remove extreme values (5^{th} and 95^{th} percentiles).

Daily maximum temperature data T_{max} were obtained from Swiss Mteorological stations for the historical period (2000 – 2019). The transient meteorological data for future climate scenarios is based on the CH2018 climate projections, which uses the EURO-CORDEX models and includes time evolving (transient)simulations under different greenhouse gas scenarios (RCPs) [17]. These scenarios have been downscaled using quantile mapping methods for greater regional detail [17]. CH2018 provides data for variables like temperature, precipitation, humidity, radiation, and wind speed for various Swiss meteorological stations. For future projections the time slides (2020-2069) is selected for three Representative Concentration Pathways (RCP2.6, RCP4.5, and RCP8.5) with number of model chains 10, 13, and 26 respectively to account for climate model uncertainty.

3.1.1 Estimation of the temperature health associations

The relationship between temperature and health outcomes was modeled using a Poisson generalised linear regression model. The application of Poisson regression models in epidemiological time series studies is well-established, particularly in environmental health research examining short-term associations between exposures and health outcomes [16]. Time-series Poisson regression models have been extensively employed to evaluate exposure-mortality associations in studies of air pollution and other environmental factors [18]. This methodological approach is consistently applied across diverse research contexts, including studies examining the effects of ambient ozone on respiratory mortality, where time-series generalized additive regression models with quasi-Poisson regression are utilized to analyze associations between environmental exposures and health outcomes [19].

The daily count of deaths (mortality) or emergency hospital admissions (morbidity/EHA) on day t is denoted by the outcome Y_t. The Possion generalised linear model (GLM) links the expected count $E[Y_t]$ to predictors through a log link. The log link function in Poisson GLMs facilitates the interpretation of regression coefficients on a multiplicative scale. This property is fundamental to epidemiological practice, as it allows to express associations as relative risks or rate ratios. In environmental epidemiology, this approach enables the quantification of short-term associations between exposures and health outcomes [16].

Heat can affect health not only on the same day but also over subsequent days

(delayed effects). To capture this, we constructed lagged temperature variables, where T_t is the temperature observed on day t and $T_{t,l}$ denotes temperature l days before day t. We considered lags up to $L = 21$ days to allow for delayed impacts:

$$T_{t,l} = T_{t-l}, \quad l = 1, 2, \ldots, L \tag{3.2}$$

To summarise exposure across the lag window in a single metric, the temperature over the lag period was computed:

$$T_{combined,t} = \frac{1}{L} \sum_{l=1}^{L} T_{t,l} \tag{3.3}$$

The relationship between temperature and health outcomes is typically non-linear: risk may be lowest at moderate temperatures and increase at both high and (depending on context) low temperatures. To flexibly model such non-linear patterns without imposing a specific functional form (e.g., strictly linear or quadratic), a natural spline basis functions is usually implemented. Natural splines represent the exposure-response curve as a smooth function composed of polynomials joined at knots with additional constraints that stabilise the function in the tails. Natural splines S with $df = 3$ degrees of freedom were applied to the combined temperature reads as:

$$S(T_{combined}) = \text{bs}(T_{combined}, df = 3) \tag{3.4}$$

.

The Poisson regression model was specified as:

$$\log(E[Y_t]) = \beta_0 + \sum_{j=1}^{df} \beta_j S_j(T_{combined,t}) \tag{3.5}$$

,

where where β_0 is the intercept and β_j are coefficients associated with the spline basis functions. Because the model is fitted on the log scale, exponentiating the linear predictor yields the expected count scale and enables the derivation of relative risks. Relative risk (RR) compares the estimated risk (or rate) of the outcome at a given temperature T to the risk at a reference temperature. Under the log-link GLM, the RR associated with temperature T is calculated as:

$$RR(T) = \exp\left(\sum_{j=1}^{df} \beta_j S_j(T) \right) \tag{3.6}$$

.

The minimum morbidity/mortality temperature (MMT) is defined as the temperature at which the model implied risk is lowest. In practice, MMT is identified

by evaluating the fitted exposure response function over a fine grid of temperatures and selecting the temperature that minimises the predicted risk:

$$MMT = \arg\min_{T} Y(T) \tag{3.7}$$

Finally, we expressed all temperature-specific relative risks relative to the MMT, so that $RR = 1$ at $T = MMT$:

$$RR_{normalized}(T) = \frac{RR(T)}{RR(MMT)} \tag{3.8}$$

3.2 Attributable Fraction

3.2.1 Mortality approach

To quantify the share of deaths statistically attributable to heat exposure, we used the attributable fraction [20]. AF expresses the proportion of mortality that would be avoided if exposure were reduced to a reference level, assuming the estimated exposure–response relationship is causal and other factors remain unchanged. For mortality analysis, the attributable fraction (AF) was calculated by first identifying heat-affected days as those where at least one lagged temperature exceeded the MMT. For each heat-affected day d, the relative risk for each lag was interpolated from the RR curve:

$$RR_{d,l} = \text{interp}(T_{d,l}, T_{range}, RR_{curve}) \tag{3.9}$$

,

where temperatures outside the modeled range ($Q_{0.05}(T)$ to $Q_{0.95}(T)$) were assigned $RR = 1$, and values were capped at the maximum observed RR. The excess risk coefficient for each day was computed as the median across lags:

$$\beta_d = \text{median}_{l=1}^{L}(RR_{d,l} - 1) \tag{3.10}$$

,

The excess mortality for each heat-affected day is:

$$E_d = \beta_d \times Y_d \tag{3.11}$$

.

The total excess mortality over all heat-affected days H is:

$$E_{total} = \sum_{d \in H} E_d \tag{3.12}$$

.

The attributable fraction is calculated using the exponential formula:

$$AF = 1 - \exp\left(-\frac{E_{total}}{\sum_{d=1}^{D} Y_d}\right) \tag{3.13}$$

where D is the total number of days in the study period.

3.2.2 Morbidity approach

For morbidity analysis, a simplified approach was used where the attributable fraction was directly applied to the total morbidity count [7]:

$$AF = \frac{E_{total}}{\sum_{d=1}^{D} Y_d} \tag{3.14}$$

.

This linear approach was chosen due to the lower baseline morbidity rates in some cantons.

3.2.3 Baseline period health impacts

Heat-attributable health impacts during the baseline period (2000-2019) were calculated as:

$$Y_{baseline,heat} = AF \times \sum_{d \in baseline} Y_d \tag{3.15}$$

The annual baseline impact was computed by dividing by the number of years:

$$Y_{annual,baseline} = \frac{Y_{baseline,heat}}{N_{years}} \tag{3.16}$$

where $N_{years} = 20$ for the 2000-2019 period.

3.3 Projected mortality and morbidity

Projected health impacts were derived by (i) combining empirically estimated temperature–health relationships (expressed as relative risks RR) normalized to the historical minimum mortality/morbidity temperature MMT with (ii) daily temperature projections from multiple climate-model chains. Throughout, $Y_{baseline,daily}$ was treated as the expected mean daily health outcome under present-day conditions (estimated from the filtered historical period) and scale future impacts

relative to this baseline. Uncertainty from the climate projections is propagated by calculating quantiles across climate-model chains.

3.3.1 Mortality projections

For mortality, health impacts were calculated using the attributable fraction AF, which represents the proportion of observed (or expected) deaths that can be attributed to exposure above a reference level conditional on the estimated exposure–response function. For each future year, the future AF was calculated by first filtering future predictions to days above MMT and then by selecting the median daily RR across climate model chains as follows:

$$RR_{year,d} = \text{quantile}_{0.5}(\{RR_{year,d,m}\}_{m=1}^{M}) \tag{3.17}$$

,

followed by interpolating RR values and computing the future AF as follows:

$$AF_{future,year} = 1 - \exp\left(-\frac{\sum_{d \in H_{year}} (RR_{year,d} - 1) \times Y_{baseline,daily}}{\sum_{d \in year} Y_{baseline,daily}}\right) \tag{3.18}$$

,

where $Y_{baseline,daily}$ is the mean daily mortality from the filtered historical period. Finally, the estimated total future deaths is obtained by using the relationship:

$$Y_{future,year} = \frac{AF_{future,year} \times Y_{baseline,total}}{1 - AF_{future,year}} \tag{3.19}$$

where $Y_{baseline,total}$ is the average annual historical mortality count. Decadal totals were computed by summing annual estimates:

$$Y_{decade} = \sum_{y \in decade} Y_{future,year} \tag{3.20}$$

.

Multi-decadal were obtained in the same way, but summing across the multi year periods, e.g. 20 years.

3.3.2 Morbidity projections

For morbidity, a direct RR application was used. Daily predicted morbidity was calculated as:

$$Y_{predicted,d} = Y_{baseline,daily} \times RR_{future,d} \tag{3.21}$$

where $RR_{future,d}$ is normalized relative to the historical MMT:

$$RR_{future,d} = \frac{\exp(f(T_{future,d}))}{\exp(f(MMT_{historical}))} \tag{3.22}$$

For uncertainty quantification, the quantile q of RR across model chains was used:

$$Y_{predicted,d,q} = Y_{baseline,daily} \times \text{quantile}_q(\{RR_{future,d,m}\}_{m=1}^{M}) \tag{3.23}$$

with $q \in \{0.1, 0.5, 0.9\}$ representing the 10$^{\text{th}}$ percentile (low), 50$^{\text{th}}$ (median) and 90$^{\text{th}}$ percentile (high) estimates. The attributable fraction was incorporated by computing:

$$AF_d = \frac{RR_d - 1}{RR_d} \tag{3.24}$$

and the excess morbidity:

$$Y_{excess,d} = AF_d \times Y_{baseline,daily} \tag{3.25}$$

.

Total predicted morbidity is obtained as follows,

$$Y_{total,d} = Y_{baseline,daily} + Y_{excess,d} \tag{3.26}$$

with decadal totals computed as:

$$Y_{decade,q} = \sum_{d \in decade} Y_{predicted,d,q} \tag{3.27}$$

3.4 Adaptation scenarios

Associations between temperature and health outcomes are estimated from historical observations. In future periods, however, the heat-health relationship may change if populations adapt through a combination of physiological acclimatisation, behavioural responses (e.g., changes in activity patterns), and structural or institutional measures (e.g., cooling, heat-warning systems) [21, 9].

To represent this possibility without assuming a constant level of adaptation at all temperatures, we introduced a *temperature-dependent* adaptation function [22, 23]. This function is designed to be (i) bounded between a minimum and maximum adaptation level, (ii) increasing with temperature, and (iii) smooth, avoiding abrupt discontinuities.

We define an adaptation level $A(T) \in [A_{\min}, A_{\max}]$ that increases with daily temperature T. For temperatures below a minimum heat-relevant threshold $T_{\min}$,

adaptation is set to a low baseline value $A_{\min}$, reflecting limited acclimatisation and limited behavioural change under moderate conditions. For $T \geq T_{\min}$, $A(T)$ increases smoothly according to a logistic curve, with the strongest increase occurring around $T_{\text{threshold}}$:

$$A(T) = \begin{cases} A_{min} & \text{if } T < T_{min} \\ A_{min} + \frac{A_{max} - A_{min}}{1+\exp(-s(T-T_{threshold}))} & \text{if } T \geq T_{min} \end{cases} \tag{3.28}$$

where:

- $A_{min} = 0.2$ represents minimum adaptation effectiveness
- $A_{max} = 1.0$ represents maximum adaptation effectiveness
- $T_{min} = 25C$ is the temperature below which adaptation is minimal
- $T_{threshold} = 33C$ is the temperature at which adaptation is strongest
- $s = 0.35$ controls the smoothness of the adaptation curve

To translate $A(T)$ into a reduction of heat-related risk, we define an adaptation effect for day d as

$$\text{Adaptation\_Effect}_d = \alpha \times \rho \times A(T_d) \tag{3.29}$$

where $\alpha = 0.5$ is the adaptation effectiveness coefficient and $\rho = 1.0$ is a scaling factor for different adaptation scenarios, namely $\rho < 1$ for weaker adaptation; $\rho > 1$ for stronger adaptation).

The adapted relative risk is then obtained by applying an exponential attenuation factor to the unadapted relative risk $RR(T)$ is

$$RR_{adapted}(T) = RR(T) \times \exp(-\text{Adaptation\_Effect}) \tag{3.30}$$

This formulation preserves positivity of relative risks and implements adaptation as a multiplicative reduction on the log-risk scale. For future projections with adaptation, the MMT from the historical period (before adaptation) was used to normalize:

$$RR_{adapted,normalized}(T) = \frac{RR_{adapted}(T)}{RR_{historical}(MMT)} \tag{3.31}$$

3.5 Uncertainty quantification

Uncertainty in future projections arises from climate model uncertainty and RR estimation uncertainty. For each RCP scenario and decade, we report:

$$Y_{decade} = \text{quantile}_{0.5}(\{Y_{decade,m}\}_{m=1}^{M}) \tag{3.32}$$

$$Y_{decade,low} = \text{quantile}_{0.1}(\{Y_{decade,m}\}_{m=1}^{M}) \tag{3.33}$$

$$Y_{decade,high} = \text{quantile}_{0.9}(\{Y_{decade,m}\}_{m=1}^{M}) \tag{3.34}$$

where M is the number of climate model chains for the given RCP scenario (10 for RCP2.6, 13 for RCP4.5, and 26 for RCP8.5).

Chapter 4

Results

4.1 Relative Risk and Projected Trends

The relative risk (RR) during the reference period associated with mortality is shown for four illustrative cantons for the population over 75 in Figure 4.1. This figure shows the temperature–mortality exposure response relationship for the four cantons (BS, BE, VD, ZH). In all cantons, the association follows a typical U or J shaped pattern, with the lowest relative risk occurring at the minimum mortality temperature (MMT - green dotted line) and increasing risks toward both colder and warmer temperatures.

The estimated MMT varies across cantons, ranging from 17.86 °C in ZH and 18.49 °C in BE to higher values in VD (23.36 °C) and BS (24.59 °C). This indicates substantial regional heterogeneity. The heat-related risk increases steeply above the MMT in all cantons, particularly in VD and BE, where relative risks exceed 3 at the highest observed temperatures. BS also shows a marked increase at high temperatures, though less pronounced than VD and BE. ZH exhibits the weakest heat-related gradient, with a more moderate increase in relative risk.

The projected relative risk trends (RR) associated with mortality and for people over 75 for the same illustrative cantons and averaged per decades and climate models for the three climate scenarios are shown in Figure 4.2. In all cantons, projected risks increase over time, with a clear gradient across emission scenarios. The strongest increases are consistently observed under RCP8.5, followed by RCP4.5, while RCP2.6 shows comparatively modest changes and in some cases near-stabilization over time.

The magnitude of the projected increase differs substantially across cantons. BE exhibits the largest absolute risk levels and the most pronounced upward trend, particularly under RCP8.5. VD shows moderate but steady increases across scenarios. BS and ZH display smaller absolute risk changes, although the divergence between scenarios becomes increasingly evident after mid-century. Overall, the results indicate a scenario-dependent amplification of temperature-related

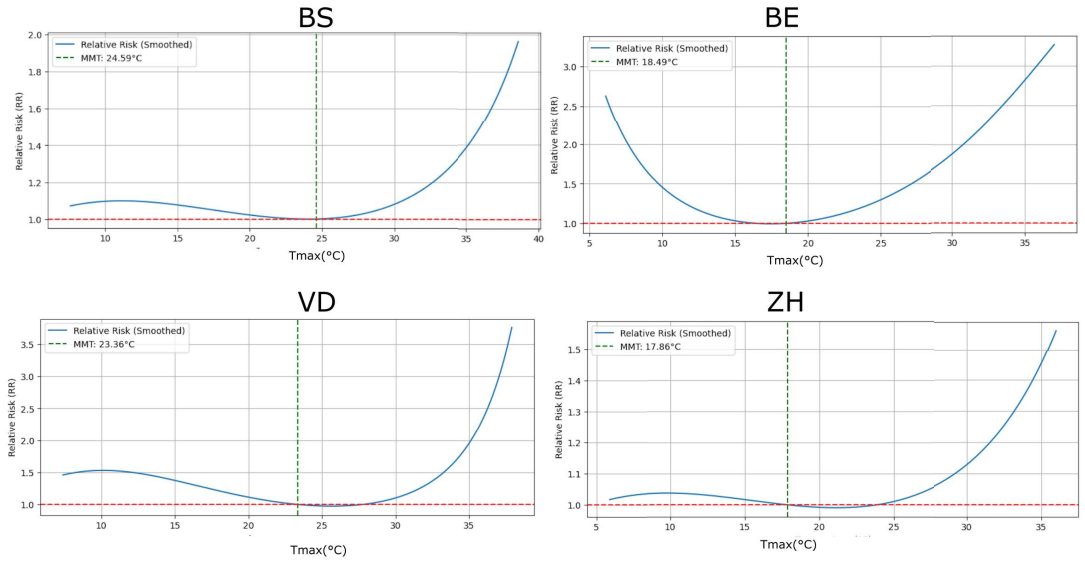


Figure 4.1: **Smoothed relative risks (RR) of mortality are shown as a function of daily maximum temperature**. The green dashed vertical line indicates the minimum mortality temperature (MMT) for each canton, and the red dashed horizontal line represents $RR = 1$ (reference risk). The cantons are from top clockwise: BS=Basel Stadt, BE = Bern, VD = Vaud, ZH = Zurich.

risks, with the gap between mitigation (RCP2.6) and high-emission pathways (RCP8.5) widening toward the end of the projection period.

The relative risk (RR) during the reference period associated with emergency hospital admissions (i.e. morbidity) is shown for four illustrative cantons for the whole population in Figure 4.3. This figure presents the exposure–response relationships between daily maximum temperature (T_{max}) and EHAs in four representative Swiss cantons (Basel Stadt, Bern, Vaud, Zurich). In all cantons, the association is non-linear, with risks increasing at higher temperatures, although the magnitude and shape of the relationship vary regionally. The estimated minimum morbidity temperature (MMT) differs substantially across cantons, ranging from 15.6 °C in Zurich and 17.4 °C in VD to markedly higher values in BE (26.4 °C) and BS (26.9 °C). Above the MMT, emergency admissions increase progressively with rising T_{max}. The steepest heat-related increase is observed in Basel Stadt, where relative risks exceed 3 at the highest temperatures. Zurich also shows a pronounced heat effect, though of smaller magnitude. Bern and Vaud exhibit more moderate increases at high temperatures. At lower temperatures, morbidity risks are generally below or close to the reference level, with no strong evidence of pronounced cold-related increases.

The projected relative risk trends (RR) associated with emergency hospital admissions for all ages for the same illustrative cantons and averaged per decades and climate models for the three climate scenarios are shown in Figure 4.4. Overall, projected changes are modest in magnitude, with relative risks remaining close to 1 throughout the period. In VD and ZH, a clearer scenario gradient is visible, with slightly higher risks under RCP8.5 compared to RCP4.5 and RCP2.6 toward the end of the century. In contrast, BS and BE display a less consistent pattern, and in some periods RCP2.6 shows marginally higher values than the higher-emission scenarios. However, these differences are very small in absolute terms and fall within a narrow range of variation across decades. The apparent lack of a strong monotonic scenario gradient may reflects the relatively small projected temperature differences in the relevant exposure range. Overall, scenario-specific differences in morbidity risk remain limited in magnitude over the projection period.

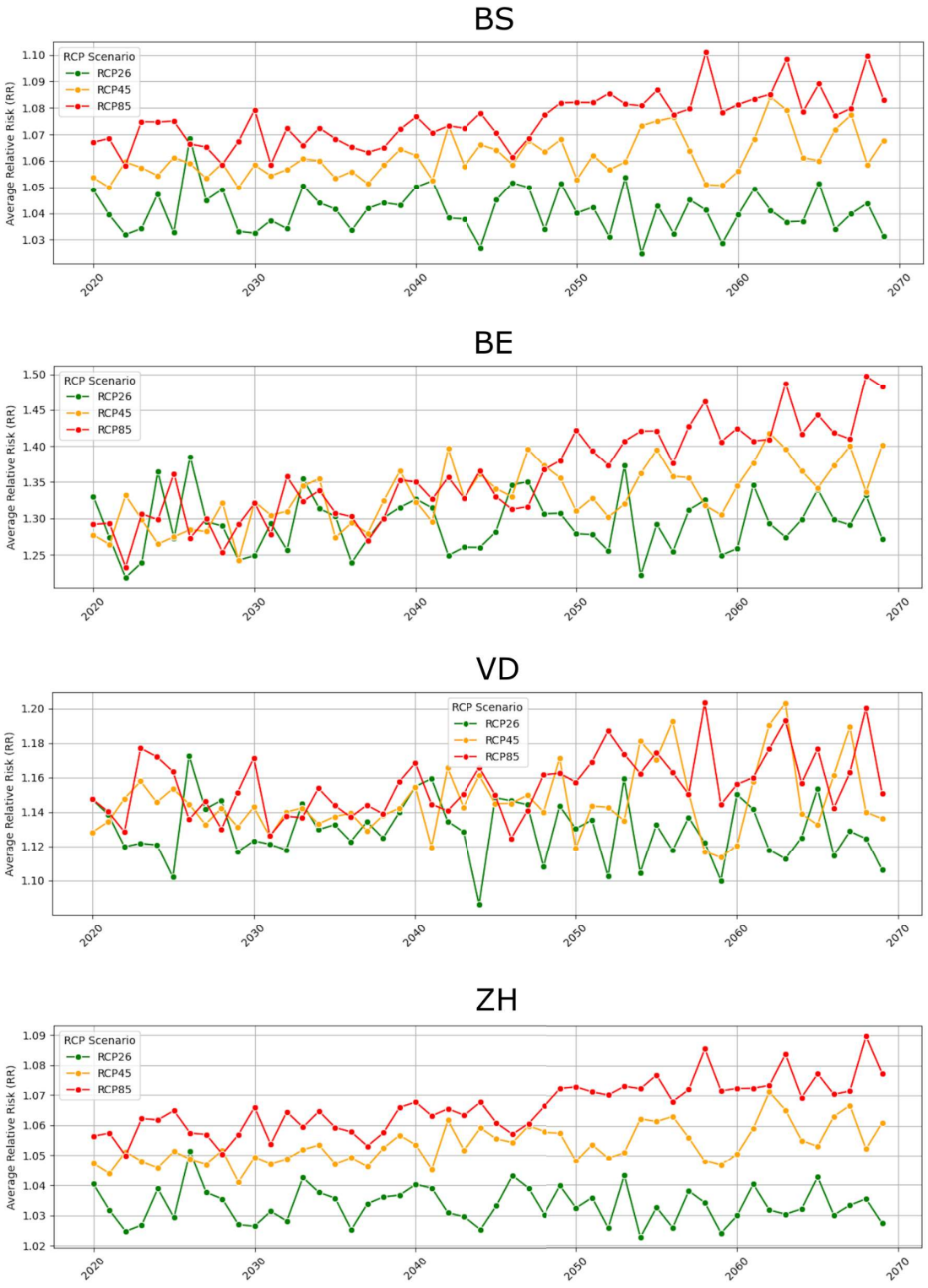


Figure 4.2: **Decade-averaged relative risk trends for mortality under different climate scenarios in four Swiss cantons (BS, BE, VD, ZH)**. Average relative risks (RR) are shown for the period 2020–2070 under RCP2.6 (green), RCP4.5 (orange), and RCP8.5 (red). Values represent decade-averaged projections. The cantons are from top to bottom: BS=Basel Stadt, BE = Bern, VD = Vaud, ZH = Zurich.

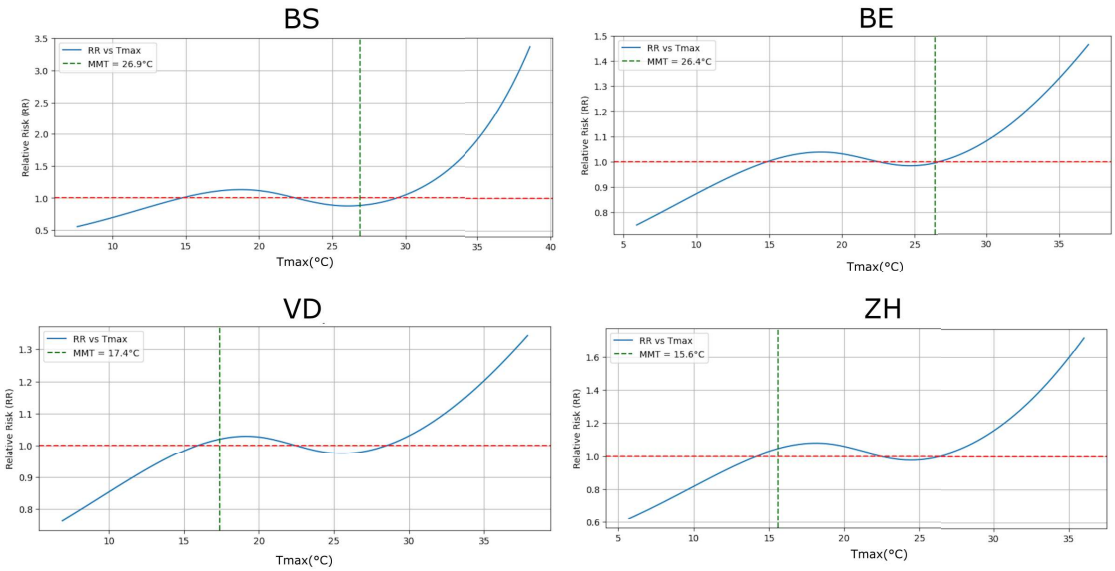


Figure 4.3: **Smoothed relative risks (RR) of morbidity are shown as a function of daily maximum temperature**. The green dashed vertical line indicates the minimum morbidity temperature (MMT) for each canton, and the red dashed horizontal line represents RR = 1 (reference risk). The cantons are from top clockwise: BS=Basel Stadt, BE = Bern, VD = Vaud, ZH = Zurich.

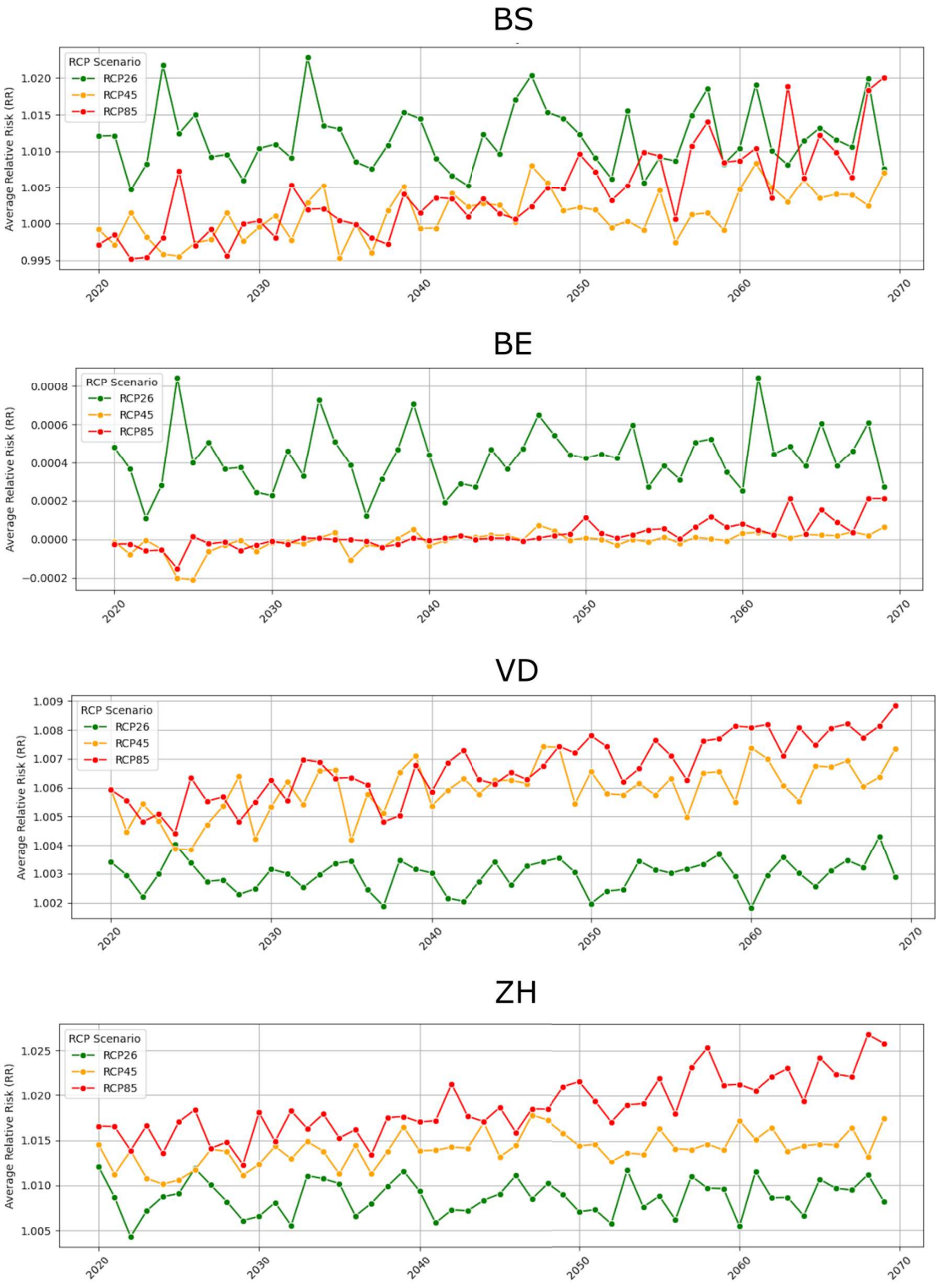


Figure 4.4: **Decade-averaged relative risk trends for morbidity under different climate scenarios in four Swiss cantons (BS, BE, VD, ZH)**. Average relative risks (RR) are shown for the period 2020–2070 under RCP2.6 (green), RCP4.5 (orange), and RCP8.5 (red). Values represent decade-averaged projections. The cantons are from top to bottom: BS=Basel Stadt, BE = Bern, VD = Vaud, ZH = Zurich.

4.2 Mortality and Morbidity counts

The number of heat-related deaths in Switzerland under three emission scenarios (RCP2.6, RCP4.5, and RCP8.5) compared with the reference period are summarised in Table 4.1. Results are stratified by age group (< 75 years and ≥ 75 years). Values in brackets indicate the uncertainty range (10^{th} and 90^{th} percentiles).

Table 4.1: **Heat related deaths stratified by age group**. Projected number of heat-related deaths (median) in Switzerland by age group under different emission scenarios. Values are cumulative counts over 20 years; brackets indicate the (10^{th} and 90^{th} percentiles.

		Heat-related deaths [10^{th}–90^{th} pct.]	
Indicator	Scenario	< 75 years	≥ 75 years
Heat-related deaths	Reference	626	4855
	RCP 2.6	1605 [871–2407]	5700 [1413–12630]
	RCP 4.5	3031 [1399–4238]	9007 [2256–11560]
	RCP 8.5	4238 [2087–7114]	11560 [2263–27550]

The results show that individuals aged ≥ 75 years are considerably more affected by heat-related mortality than those under 75 years. Absolute numbers remain markedly higher in the older age group across all scenarios. With increasing emission levels, projected deaths rise considerably in both age categories. Heat-related mortality among individuals aged <75 years is projected to increase substantially compared with the reference period across all emission scenarios. Under RCP2.6, mortality in this age group is estimated to rise to 2.56 times the reference level (10^{th} and 90^{th} percentiles: 1.39–3.85). Under RCP4.5, the increase reaches 4.84 times the reference (2.23–6.77), and under RCP8.5 up to 6.77 times the reference level (3.33–11.36). For individuals aged ≥ 75 years, projected increases are more moderate in relative terms but remain considerable in absolute burden. Mortality in this age group is projected to increase to 1.17 times the reference level under RCP2.6 (0.29–2.60), 1.86 times under RCP4.5 (0.46–2.38), and 2.38 times under RCP8.5 (0.47–5.67). All emission scenarios are associated with considerable uncertainty, reflected in the wide spread between lower and upper percentiles. The uncertainty range expands with increasing emission levels. The wider uncertainty range observed for the ≥ 75 age group likely reflects the higher baseline mortality and stronger temperature sensitivity in this population. Heat-related deaths are estimated by applying the exposure–response function to baseline mortality under projected temperature conditions. Because mortality rates

are substantially higher in older adults and the temperature–mortality relationship tends to be steeper in this age group, uncertainty in the exposure–response estimates and in projected temperatures is amplified when translated into attributable deaths. As a result, small variations in projected heat exposure can lead to comparatively larger variation in estimated deaths producing a wider 10th–90th percentile range. Further to the age stratified mortality counts, the RR for the aggregated age group was used to derive the aggregated mortality. Since the exposure-response relation is derived for all age group, the final count does not correspond to the count separated by age group and then aggregated. This is because the models are fitted to different data slices, and they are not expected to match. This model was finally used to calculate the effect of adaptation following the approach in Section 3.4. Results are shown in Table 4.2. Without adaptation, projected mortality increases substantially compared with the reference period, reaching 7846 deaths under RCP2.6, 13330 under RCP4.5, and 17755 under RCP8.5 (cumulative values over 20 years). The associated uncertainty ranges are wide and expand under higher emission pathways. When adaptation is incorporated into the projections, the estimated number of heat-related deaths is markedly reduced across all scenarios. Under RCP2.6, projected deaths decrease approx. 4 times, approx. 5 times under RCP4.5 , and approx. 8 times under RCP8.5 in the median. Although substantial uncertainty remains, these results suggest that adaptation measures could considerably mitigate the future burden of heat-related mortality, even under high-emission scenarios.

Table 4.2: **Heat related deaths aggregated**. Projected heat-related deaths in Switzerland for all age groups combined under RCP2.6, RCP4.5 and RCP8.5. Results are shown without adaptation and with adaptation. Values represent cumulative deaths over 20 years (2050–2069) compared with the reference period (2000–2019). Brackets indicate the (10^{th} and 90^{th} percentiles uncertainty range.

		Heat-related deaths [10^{th}–90^{th} pct.]	
Indicator	Scenario	All ages	All ages with adaptation
Heat deaths	Ref.	5116	–
	RCP2.6	7846 [3380–15962]	1996 [1834–2900]
	RCP4.5	13330 [5635–29893]	2509 [1995–4796]
	RCP8.5	17755 [7546–37987]	2150 [1802–6929]

The number of heat-related emergency hospital admissions (EHAs) in Switzerland under three emission scenarios (RCP2.6, RCP4.5, and RCP8.5) compared with the reference period are summarised in Table 4.3. Results are stratified by age group as follows: 0-14, 15-64, 65-74, 75+ years. Values in brackets indicate the uncertainty range (10^{th} and 90^{th} percentiles). Relative to the reference period, pro-

Table 4.3: **Heat-related emergency hospital admissions (EHA) by age group**. Heat-related emergency hospital admissions (EHA) by age group for the reference period and projected under climate scenarios RCP 2.6, RCP 4.5 and RCP 8.5. Values are point estimates; bracketed values indicate the low–high percentile range, shown on a second line within each cell.

		Heat-related EHA [10^{th}–90^{th} pct.]			
Indicator	Scenario	<14 years	15–64 years	65–74 years	≥ 75 years
Heat-related EHA	Reference	94	18880	1458	3712
	RCP 2.6	162 [159–164]	20417 [19982–21627]	1639 [1619–1656]	4068 [3999–4212]
	RCP 4.5	162 [159–165]	20555 [20077–21124]	1641 [1622–1658]	4072 [3992–4163]
	RCP 8.5	163 [159–165]	20703 [20198–21688]	1643 [1624–1659]	4092 [4010–4227]

jected heat-related emergency hospital admissions increase across all age groups under every RCP. For children <14 years, admissions in the median rise to 1.72 times the reference level under RCP 2.6 and RCP 4.5, and to 1.73 times under RCP 8.5. For adults 15–64 years, admissions increase more modestly to 1.08 times (RCP 2.6), 1.09 times (RCP 4.5), and 1.10 ties (RCP 8.5) the reference. For 65–74 years, admissions reach 1.12 times, 1.13 times, and 1.13 times the reference under RCP 2.6, 4.5, and 8.5, respectively. For the oldest group (over 75 years), admissions increase to 1.10 the reference under RCP 2.6 and RCP 4.5, and to 1.10 times (slightly higher) under RCP 8.5. The largest relative increase is consistently observed in the 0-14 years group, while differences between RCPs are comparatively small for the adult and older age groups.

Further to the age stratified heat-related emergency hospital admissions, the RR for the aggregated age group was used to derive the aggregated counts of emergency hospital admissions. Since the exposure-response relation is derived for the aggregated ages, the final count does not correspond to the count separated by age group and then aggregated. This model was finally used to calculate the effect of adaptation following the approach in Section 3.4. Results are shown in Table .

Across all age groups, the reference level of heat-related emergency hospital admissions (EHA) is 17664. Without adaptation, projected admissions increase to 1.09 in the median under RCP 2.6 and about 1.10 under RCP4.5 and RCP8.5. With adaptation, heat related EHA are reduced 1.14 times in RCP2.6, 1.15 times under RCP4.5 and 1.17 times under RCP8.5. These results indicates that adaptation can offsets the climate-driven increases in emergency hospital admissions, but also that the effect is considerably less pronounced than in the mortality case and than

Table 4.4: **Heat-related emergency hospital admissions (EHA) aggregated**. Heat-related emergency hospital admissions (EHA) for all age groups under the reference period and climate scenarios (RCP 2.6, RCP 4.5, RCP 8.5), shown without and with adaptation. Bracketed values indicate the low–high percentile range.

Indicator	Scenario	All age groups	
		without adaptation	with adaptation
Heat-related EHA	Reference	17664	
	RCP 2.6	19208 [18691–19999]	16723 [15093–17780]
	RCP 4.5	19367 [18823–19882]	16703 [14597–17691]
	RCP 8.5	19511 [18946–20147]	16623 [14174–17892]

differences between climate scenarios remain very minor.

Chapter 5

Discussion

This study estimates how heat-related mortality and emergency hospital admissions (EHA/morbidity) in Switzerland may change under climate change, and explores a stylised adaptation formulation that attenuates heat-related risks at higher temperatures. The approach combines (i) empirically estimated temperature–health relationships from historical data, (ii) transient daily temperature projections from multiple climate-model chains, and (iii) reporting uncertainty as percentile ranges across model chains. Result points at a scenario-dependent increase in heat-related health burden, with stronger increases for mortality than morbidity, and a pronounced concentration of mortality impacts among older adults (over 75) and morbidity effect for youngest age group (0-14).

Over the 20-year future period 2050–2069, heat-related deaths for all ages increases in the median progressively from RCP2.6 to RCP8.5 (all without adaptation), with 10^{th} and 90^{th} percentile ranges that expand under higher emissions. Age-stratified mortality results show that the ≥ 75 group dominates the absolute number of heat-attributable deaths in every scenario. Relative increases are large in both groups, and uncertainty is especially wide for $\geq$75. Whereas there is uncertainty in the absolute values, the increasing trends at increasing warming confirm findings of other studies looking at the association of temperature with heat related outcomes [24, 25, 11]. All-age heat-related EHA increase from 17664 in the reference period to 19208 (RCP2.6), 19367 (RCP4.5), and 19511 (RCP8.5), roughly a 9–10% increase overall, with small differences across RCPs. Age-stratified EHA show the largest relative change in the 0–14 group (from 94 to approx 162-163), while the largest absolute totals are in adults 15–64.Previous studies linking rising temperatures to heightened child vulnerability have suggested that children's greater exposure outdoors and higher physiological susceptibility may help explain this increase [26, 27].

The steep increase in heat-attributable deaths is consistent with more frequent/higher heat exposure in a warming climate and a non linear exposure response curve that can become steep in the upper tail. The dominance of older adults in

absolute mortality burden is also consistent with higher baseline risk and vulnerability at older ages [20, 24]. In contrast, EHA projections are comparatively flat across scenarios. Some of this may reflect genuine differences, i.e. mortality may respond more sharply to extreme heat than all-cause emergency admissions. The limited scenario separation for EHA may also reflect the fact that emergency admissions aggregate many causes and behaviours, and heat effects may be diluted when not modelled for heat-sensitive diagnoses specifically; additionally, choices around temperature metrics, trimming extremes, and attribution methods can dampen differences between scenarios.

Using the median estimates, the inclusion of adaptation substantially reduces projected heat-related mortality across all emission scenarios. Under RCP2.6, adaptation lowers cumulative deaths from 7846 to 1996, corresponding to a reduction of approximately 75%. Under RCP4.5, projected deaths decline from 13330 to 2509, representing a reduction of about 81%. The largest relative effect is observed under RCP8.5, where deaths decrease from 17755 to 2150, equivalent to a reduction of nearly 88%. For EHA, adaptation reduces totals to around 16623–16723, i.e., below the reference level and about 13–15% lower than the no-adaptation projections.

Adaptation is shown to be important for heat health outcomes, but the magnitude should be treated as illustrative rather than predictive. The adaptation formulation is deliberately stylised (i.e. logistic increase of "adaptation level" with temperature, translated into a multiplicative attenuation of RR). It shows that if adaptation were strong and increasingly effective at higher temperatures, a large share of future heat burden could be avoided [14, 11, 9]. However, because the parameters are not calibrated to measured intervention effectiveness in Switzerland, the adaptation results are best interpreted as a sensitivity experiment: "what would happen if heat risk were attenuated in this structured way?" rather than "what will happen".

This study also present some limitations driven by practical choices and available data. The report uses a distributed-lag framework and non-linear exposure–response functions estimated via Poisson regression with spline terms, then applies these relationships to transient CH2018 scenario temperatures to derive future impacts. The overall approach is consistent with established climate–health impact assessment practice: (i) estimate an empirical temperature–health association, (ii) define a reference (MMT), and (iii) combine it with scenario-based future temperatures. That said, several modelling choices materially influence interpretability.

The implementation uses a lag window (up to 21 days) but then collapses lagged exposure into a single mean temperature metric for the exposure–response fit, rather than modelling a full temperature-by-lag response surface. This is a pragmatic simplification, but it can mask important dynamics such as acute heat effects within 0–3 days and potential mortality displacement, or differences be-

tween short and longer lags. A full DLNM "cross-basis" approach would generally provide a richer and more standard treatment of distributed lag non-linearity.

The filtering strategy exluded values outside the 10th–90th percentile and temperature outside the 5th–95th percentile reduces the influence of outliers, but it also removes precisely those extremes that may be most relevant for heat-risk estimation—particularly for mortality during severe heatwaves. This can affect both the shape of the right tail of the exposure–response function and the magnitude of projected impacts in high-warming scenarios.

Adaptation modelling is stylised. The adaptation scenario is represented via a logistic temperature-dependent function that attenuates risk multiplicatively. This provides a transparent and controllable way to explore sensitivity, but it is not directly tied to specific interventions (e.g., heat–health action plans, housing retrofits, warning systems) or to observed adaptation trends. Consequently, results should be interpreted as "what-if" sensitivity analysis rather than forecasts of achievable adaptation benefits.

The report propagates climate model uncertainty using ensembles of model chains for each RCP and summarises results with 10th/50th/90th percentiles. This is a strong feature of the analysis. However, the uncertainty ranges shown, especially for mortality, are also shaped by: (i) the steepness of the fitted exposure–response tail, (ii) the treatment of temperatures outside the modelled range (assigning RR=1 and capping), and (iii) the fixed-baseline health counts used in projections. These sources can either compress or inflate uncertainty depending on how they interact with extremes, and they are distinct from the climate model spread itself.

Chapter 6

Conclusions

The projected mortality counts indicate that, without adaptation, heat-related deaths increase markedly in the future, especially under higher emissions. Age stratification shows that the over 75 group carries the dominant absolute burden across all scenarios, consistent with well-established heat vulnerability in older populations. At the same time, relative increases are also substantial in the younger age category, indicating that rising exposure can expand the burden beyond the oldest ages under increasing warming.

Projected heat-related emergency hospital admissions increase only slightly under all RCPs. This divergence between mortality and morbidity projections is an important finding: it implies that the future health burden may be dominated by severe outcomes (deaths), or that morbidity impacts may be harder to detect with the present modelling choices and data aggregation. This is due in part to the fact that only emergency hospital admissions are considered which most likely represent only the acute cases. It may also reflect outcome-specific sensitivity: emergency admissions include a broad mixture of diagnoses and ages, and short-term displacement, healthcare-seeking behaviour, and coding practices can dampen signal relative to mortality.

Finally, the adaptation scenarios substantially change the projected burden. Under the chosen adaptation formulation, adaptation strongly reduces projected heat-related deaths and also reduces projected morbidity, in some cases offsetting the climate-driven increase. This highlights a critical policy implication: projections are not purely a function of climate trajectories; they are highly sensitive to how human systems respond and the speed of such responses. Yet, data are not readily available to assess the potential effect of adaptation measures and whether reduction in health burden can be attributable to discrete adaptation responses and their combination.

The main conclusions are outlined as follows:

- Heat-related mortality increases substantially under climate change, with a clear gradient across emission scenarios and pronounced impacts among

older adults (75 years). The results indicate that high-emission pathways lead to much larger cumulative mortality burdens than strong mitigation scenarios.

- Heat-related emergency hospital admissions increase more modestly than mortality in the presented projections, with relatively small differences across scenarios. This may reflect genuine outcome-specific sensitivity, but it may also be influenced by data aggregation and modelling choices that dampen extremes or dilute signal.

- Adaptation assumptions are pivotal. Under the stylised adaptation function used here, projected burdens can be markedly reduced, in some cases offsetting climate-driven increases. This highlights that public health outcomes depend strongly on the pace and effectiveness of adaptation, not just on climate trajectories. While adaptation improvement to the stylised case are needed to have results that are linked to intervention evidence, such evidence is currently largely missing.

- This study also present a number of limitatons. It follows standard climate–health impact assessment practice by estimating a non-linear temperature–health relationship with a distributed-lag Poisson model and applying it to CH2018 scenario temperatures, but several practical choices limit interpretation. Collapsing lagged exposure into a single mean-temperature metric (instead of a full DLNM cross-basis) may obscure short-term heat effects and mortality displacement, while filtering to central temperature percentiles reduces outliers but also removes the extremes most relevant for heatwave mortality, potentially dampening impacts in high-warming scenarios. Adaptation is represented with a stylised logistic risk-reduction function, so results should be read as sensitivity "what-if" scenarios rather than intervention-based forecasts. Although climate-model uncertainty is well captured using ensemble chains and percentile summaries, the reported uncertainty ranges are also influenced by modelling decisions such as tail steepness, capping/extrapolation rules, and fixed baseline health counts, not just the climate spread.

Bibliography

[1] Jean-Marie Robine et al. "Death toll exceeded 70,000 in Europe during the summer of 2003". en. In: *Comptes Rendus. Biologies* 331.2 (Dec. 2007), pp. 171–178. ISSN: 1631-0691, 1768-3238. DOI: 10.1016/j.crvi.2007.12.001. URL: https://comptes-rendus.academie-sciences.fr/biologies/articles/10.1016/j.crvi.2007.12.001/ (visited on 01/08/2026).

[2] Joan Ballester et al. "Heat-related mortality in Europe during the summer of 2022". en. In: *Nature Medicine* 29.7 (July 2023), pp. 1857–1866. ISSN: 1078-8956, 1546-170X. DOI: 10.1038/s41591-023-02419-z. URL: https://www.nature.com/articles/s41591-023-02419-z (visited on 01/08/2026).

[3] Elisa Gallo et al. "Heat-related mortality in Europe during 2023 and the role of adaptation in protecting health". en. In: *Nature Medicine* 30.11 (Nov. 2024), pp. 3101–3105. ISSN: 1078-8956, 1546-170X. DOI: 10.1038/s41591-024-03186-1. URL: https://www.nature.com/articles/s41591-024-03186-1 (visited on 01/08/2026).

[4] Tomáš Janoš et al. "Heat-related mortality in Europe during 2024 and health emergency forecasting to reduce preventable deaths". en. In: *Nature Medicine* 31.12 (Dec. 2025), pp. 4065–4074. ISSN: 1078-8956, 1546-170X. DOI: 10.1038/s41591-025-03954-7. URL: https://www.nature.com/articles/s41591-025-03954-7 (visited on 01/08/2026).

[5] Ana M Vicedo-Cabrera et al. "The footprint of human-induced climate change on heat-related deaths in the summer of 2022 in Switzerland". In: *Environmental Research Letters* 18.7 (July 2023), p. 074037. ISSN: 1748-9326. DOI: 10.1088/1748-9326/ace0d0. URL: https://iopscience.iop.org/article/10.1088/1748-9326/ace0d0 (visited on 01/08/2026).

[6] David García-León et al. "Temperature-related mortality burden and projected change in 1368 European regions: a modelling study". en. In: *The Lancet Public Health* 9.9 (Sept. 2024), e644–e653. ISSN: 24682667. DOI: 10.1016/S2468-2667(24)00179-8. URL: https://linkinghub.elsevier.com/retrieve/pii/S2468266724001798 (visited on 01/08/2026).

[7] Florian Schulte, Martin Röösli, and Martina S. Ragettli. "Risk, Attributable Fraction and Attributable Number of Cause-Specific Heat-Related Emergency Hospital Admissions in Switzerland". In: *International Journal of Public Health* 69 (Oct. 2024), p. 1607349. ISSN: 1661-8564. DOI: 10.3389/ijph.

2024.1607349. URL: https://www.ssph-journal.org/articles/10.3389/ijph.2024.1607349/full (visited on 01/08/2026).

[8] Martina S. Ragettli et al. "Vulnerability to heat-related mortality and the effect of prevention measures: a time-stratified case-crossover study in Switzerland". In: *Swiss Medical Weekly* 154.10 (Oct. 2024), p. 3410. ISSN: 1424-3997. DOI: 10.57187/s.3418. URL: https://smw.ch/index.php/smw/article/view/3418 (visited on 01/09/2026).

[9] B. Bednar-Friedl et al. "Europe". In: *Climate Change 2022: Impacts, Adaptation and Vulnerability. Contribution of Working Group II to the Sixth Assessment Report of the Intergovernmental Panel on Climate Change*. Ed. by H.-O. Pörtner et al. Cambridge, UK and New York, NY, USA: Cambridge University Press, 2022, pp. 1817–1927. DOI: 10.1017/9781009325844.015.

[10] Martina S. Ragettli and Martin Röösli. "Hitze-Massnahmen-Toolbox: Ein Massnahmenkatalog für den Schutz der menschlichen Gesundheit vor Hitze". In: (2021).

[11] Fiona Federer et al. "Exploratory modeling and analysis of adaptation to urban heat stress under climate change in Switzerland". en. In: *Urban Climate* 65 (Feb. 2026), p. 102729. ISSN: 22120955. DOI: 10.1016/j.uclim.2025.102729. URL: https://linkinghub.elsevier.com/retrieve/pii/S2212095525004456 (visited on 01/26/2026).

[12] Aleš Urban et al. "The effectiveness of heat prevention plans in reducing heat-related mortality across Europe". In: *Environmental Research Letters* 20.12 (Dec. 2025), p. 124071. ISSN: 1748-9326. DOI: 10.1088/1748-9326/ae2775. URL: https://iopscience.iop.org/article/10.1088/1748-9326/ae2775 (visited on 01/10/2026).

[13] Saeid Vaghefi et al. *Quantifying the Financial Burden of Heat-Related Hospital Admissions in Switzerland under a Changing Climate: A Scalable Analytical Framework*. 2025. DOI: 10.2139/ssrn.5351390. URL: https://www.ssrn.com/abstract=5351390 (visited on 01/10/2026).

[14] Benedikt Wicki et al. "Socio-environmental modifiers of heat-related mortality in eight Swiss cities: A case time series analysis". en. In: *Environmental Research* 246 (Apr. 2024), p. 118116. ISSN: 00139351. DOI: 10.1016/j.envres.2024.118116. URL: https://linkinghub.elsevier.com/retrieve/pii/S0013935124000203 (visited on 01/12/2026).

[15] Martina S. Ragettli et al. "Exploring the association between heat and mortality in Switzerland between 1995 and 2013". In: *Environmental Research* 158 (2017), pp. 703–709. ISSN: 0013-9351. DOI: https://doi.org/10.1016/j.envres.2017.07.021. URL: https://www.sciencedirect.com/science/article/pii/S0013935116309537.

[16] A. Gasparrini, B. Armstrong, and M. G. Kenward. "Distributed lag non-linear models". In: *Statistics in Medicine* 29.21 (2010), pp. 2224–2234. DOI: https://doi.org/10.1002/sim.3940.

[17] CH2018 Project Team. *CH2018 – Climate Scenarios for Switzerland. Technical Report*. https://www.nccs.admin.ch/ch2018/en.html. National Centre for Climate Services (NCCS), Zurich. ISBN: 978-3-9525031-4-0. 2018.

[18] Chengyuan Lu, Jelle J. Goeman, and Hein Putter. "Maximum Likelihood Estimation in the Additive Hazards Model". In: *Biometrics* (2022). DOI: 10.1111/biom.13764.

[19] Aurelio Tobías, Yoonhee Kim, and Lina Madaniyazi. "Time-Stratified Case-Crossover Studies for Aggregated Data in Environmental Epidemiology: A Tutorial". In: *International Journal of Epidemiology* (2024). DOI: 10.1093/ije/dyae020.

[20] Pierre Masselot et al. "Estimating future heat-related and cold-related mortality under climate change, demographic and adaptation scenarios in 854 European cities". en. In: *Nature Medicine* 31.4 (Apr. 2025), pp. 1294–1302. ISSN: 1078-8956, 1546-170X. DOI: 10.1038/s41591-024-03452-2. URL: https://www.nature.com/articles/s41591-024-03452-2 (visited on 01/12/2026).

[21] Veruska Muccione et al. "Towards a more integrated research framework for heat-related health risks and adaptation". en. In: *The Lancet Planetary Health* 8.1 (Jan. 2024), e61–e67. ISSN: 25425196. DOI: 10.1016/S2542-5196(23)00254-1. URL: https://linkinghub.elsevier.com/retrieve/pii/S2542519623002541 (visited on 01/12/2026).

[22] Christopher W. Callahan, Jordan Trok, A. J. Wilson, et al. "Increasing risk of mass human heat mortality if historical weather patterns recur". In: *Nature Climate Change* 16 (2026), pp. 26–32. DOI: 10.1038/s41558-025-02480-1. URL: https://doi.org/10.1038/s41558-025-02480-1.

[23] Masna Rai et al. "Future temperature-related mortality considering physiological and socioeconomic adaptation: a modelling framework". In: *The Lancet Planetary Health* 6.10 (2022), e784–e792. ISSN: 2542-5196. DOI: https://doi.org/10.1016/S2542-5196(22)00195-4. URL: https://www.sciencedirect.com/science/article/pii/S2542519622001954.

[24] Evan De Schrijver et al. "Nationwide projections of heat- and cold-related mortality impacts under various climate change and population development scenarios in Switzerland". In: *Environmental Research Letters* 18.9 (Sept. 2023), p. 094010. ISSN: 1748-9326. DOI: 10.1088/1748-9326/ace7e1. URL: https://iopscience.iop.org/article/10.1088/1748-9326/ace7e1 (visited on 01/08/2026).

[25] Kristie L Ebi et al. “Burning embers: synthesis of the health risks of climate change”. In: *Environmental Research Letters* 16.4 (Apr. 2021), p. 044042. ISSN: 1748-9326. DOI: 10.1088/1748-9326/abeadd. URL: https://iopscience.iop.org/article/10.1088/1748-9326/abeadd (visited on 01/12/2026).

[26] Alexander Azan et al. “Exceeding the Limits of Paediatric Heat Stress Tolerance: The Risk of Losing a Generation to Climate Inaction”. In: *BMJ Paediatrics Open* (2025). DOI: 10.1136/bmjpo-2024-002883.

[27] Caroline J. Smith. “Pediatric Thermoregulation: Considerations in the Face of Global Climate Change”. In: *Nutrients* (2019). DOI: 10.3390/nu11092010.